EFFECT OF CHARACTERISTICS OF DYNAMIC MUSCLE CONTRACTION ON CROSSTALK IN SURFACE ELECTROMYOGRAPHY RECORDINGS

S. Viljoen*, T. Hanekom* and D. Farina**

**Department of Electrical, Electronic and Computer Engineering, University of Pretoria, Pretoria, South Africa*

***Center for Sensory-Motor Interaction (SMI), Department of Health Science and Technology, Aalborg University, Aalborg, Denmark*

Abstract: An investigation into the ability of different spatial filters to reduce the amount of crosstalk in a surface electromyography measurement was conducted. A simulation model was implemented to compare the performance of four spatial filters under dynamic muscle contractions. Two parameters of a dynamic muscle contraction, namely muscle shortening and varying contraction force, were evaluated separately. The normal double differential filter resulted in the best crosstalk rejection for varying contraction force simulations, while the double differential filter performed best when incorporating muscle shortening. It is furthermore suggested that crosstalk is influenced more by muscle shortening than by changes in the contraction force.

Key words: Surface electromyography, modelling, crosstalk, analytical model, spatial filters, motor unit action potential, average rectified value, mean power spectral frequency, muscle shortening, muscle contraction.

1. INTRODUCTION

In surface electromyography (sEMG) recordings, crosstalk is the unwanted signal component detected above one muscle but generated by another muscle [1, 2]. It is one of the main areas of research in sEMG measurements [3]. Crosstalk has been investigated by experimental [1, 3 - 5] and modelling [3, 4, 6 - 8] studies. It has been shown that crosstalk signals consist mainly of far-field potentials that are generated due to the extinction of the action potential at the muscle fibre endings (end-of-fibre effect) [2 – 4, 6, 9, 10, 11]. Crosstalk depends on many anatomical and physical factors of the sEMG generation system [7, 8, 12].

Crosstalk has mainly been investigated in isotonic, isometric contractions, e.g. an evaluation of methods to reduce crosstalk [6] and a comparison of the different methods employed to quantify crosstalk [4]. This eliminates some inherent sources of crosstalk (e.g. sliding of muscles under skin). Everyday tasks, however, require dynamic muscle contractions. The objective of this study was to investigate, by simulation, the effect of some parameters of dynamic muscle contraction on crosstalk.

In a dynamic contraction the muscle shortens and the force may vary over a large range. These two parameters (degree of shortening and force) were evaluated separately to examine their individual effects on crosstalk. The geometrical changes incorporated include a change in muscle length (concentric contraction) and the accompanying change in limb radius. The performance of four spatial filters with respect to crosstalk rejection was compared for the simulated conditions.

2. METHODS

2.1 Volume conductor model

The analytical model developed by [13] was used to generate single fibre action potentials (SFAPs). A spatio-temporal function describes the generation, propagation and extinction of the SFAP. The model describes a cylindrical layered volume conductor with bone, muscle, fat, and skin tissues [13]. The layers are anisotropic and their effect on the SFAP is modelled as a two-dimensional spatial filter. A specific part of the muscle region comprises the active muscle fibres. The active muscle territory was described as an ellipse. The parameters that were fixed in the volume conductor model are reported in Table I. These include the physiological cross-sectional area (PCSA) and maximum voluntary contraction (MVC) of the muscle.

2.2 Detection system

Detection system is the general term used to refer to the electrode arrangements used to realise the spatial filters shown in Figure 2. Ten detection systems were placed circumferentially around the surface of the volume conductor with their centres in the range 0° - 45°, where 0 ° is the position directly above the muscle (see Figure 1).

Four spatial filters, with inter-electrode distance (IED) 5 mm, were considered (Figure 2): monopolar (Mono),

normal double differential (NDD). The detection points were halfway between the innervation zone (IZ) and the tendon region. The end-of-fibre effect is visible as a small bump at the end of each potential.

Table I: Fixed parameters in volume conductor model.

Parameter	Value	Reference
Bone radius	15 mm	[14]
Skin thickness	1 mm	[15]
Fibres / MU	50 – 1000	[16]
MU / muscle	200	[16]
Fibre density	20 fibres/mm²	Computed
Conductivity of skin	1 S/m	[17]
Conductivity of bone (isotropic)	0.02 S/m	[17]
Conductivity of fat (isotropic)	0.05 S/m	[18, 19]
Conductivity of muscle (radial + angular)	0.1 S/m	[18, 19]
Conductivity of muscle (longitudinal)	0.5 S/m	[18, 19]
Inter-electrode distance	5 mm	Selected
PCSA of selected muscle	600 mm²	[20]
% MVC where recruitment stops	85%	Selected
Interpulse interval variability	15%	Selected
Variation in discharge rate with force (*var_dis*)	15%	Selected

2.3 Motor unit

The SFAPs were summed together to obtain the motor unit action potentials (MUAPs). The MU territories were circular with centres located randomly within the active muscle. Each MU was assigned a specific conduction velocity (CV). CV values were limited in the range 2-7 m/s and were assigned in agreement to the size principle, i.e., CV increased with MU size [21].

2.4 Motor unit firing patterns

The firing pattern computations are based on the model developed in [22]. The MUs were recruited on the basis of MU recruitment threshold, defined by:

$$RTE(i) = e^{\ln(RR)i/n}, i = 1,2,3...n \qquad (1)$$

where RR is the % maximum voluntary contraction (MVC) where the complete MU pool is recruited. It is MVC in 3 s. The time at which a certain contraction force is reached, $t_{\%MVC}$, can thus be found from:

$$t_{\%MVC} = \frac{\%MVC}{100} \cdot 3 \qquad (2)$$

The time at which a certain MU is recruited is defined by:

$$t_{rec}(i) = t_{\%MVC} - \frac{RTE(i)}{100} \cdot t_{MVC}. \qquad (3)$$

MUs with negative t_{rec} values are not yet recruited at the time that the desired contraction strength is reached. Their discharge rate is thus set equal to zero. A discharge rate is computed for every MU with a positive recruitment time from Equation 4:

$$f_{rate}(i) = f_{\min} + var\_dis \cdot (100 - RTE(i)) \qquad (4)$$

with f_{min} = 8 pulses per second (pps) and *var_dis* the variation in discharge rate with force equal to 0.3 pps/%MVC. The discharge rates were limited to 35 pps. All the parameters correspond to experimental measurements [23].

2.5 Signal analysis

The average rectified value (ARV) and mean power spectral frequency (MNF) are commonly used to evaluate the characteristics of surface EMG [1, 2]. The ARV is equal to the area under the rectified signal. Its value will increase and then decrease with increasing electrode separation. The slope of the decrease provides an indication of filter selectivity with respect to crosstalk. The propagating components, which form the main part of an EMG signal, are attenuated rapidly with increasing distance. Crosstalk signals propagate with less attenuation and can thus be measured a larger distance from their origin [11]. The detection system which shows the best suppression of amplitude content with increasing distance will thus be preferential for crosstalk reduction.

The MNF value defines the frequency component that carries the largest weight (centre of gravity). It thus provides information about the frequency content of the crosstalk signal [1, 2]. The interpretation of the MNF is based on the fact that the filtering properties of a detection system are determined by its transfer function. The sEMG waveform is time and space dependent. Since the electrode separation and location are spatial parameters, they influence the spatial filtering characteristics of the electrode configuration. The temporal and spatial waveforms are linked via the CV of the muscle fibres. A change in the spatial characteristics of the electrode configuration will thus also be reflected in the temporal waveform as a filtering effect where the relative contributions of the frequency components are weighted relative to those of the original signal.

Typically, the MNF will increase with increasing electrode separation. The reason behind this is than an increase in electrode separation leads to a larger pick-up area, which in turn increases the crosstalk [4]. The effect of electrode location on the MNF is determined by the main contributors to the sEMG signal at that location, i.e. whether the MNF will increase or decrease with increasing interelectrode distance depends on the relative contributions of the propagating and non-propagating components. For example, if the electrode system is located close to the tendon, an increase in the MNF can be expected relative to the MNF observed for a detection system location midway between the tendon and IZ because the non-propagating components of the signal originating at this location contribute more to the detected waveform than the components of the true EMG signal [3].

The ARV and MNF were computed from 1 s long simulated signals at the 10 transversal locations for each spatial filter. These variables were normalized with respect to the value assumed at the first location (0°).

2.6 Simulation of muscle shortening

Three libraries of SFAPs were created using the analytical model described above. The muscle fibre length was changed between the libraries to simulate muscle shortening. A constant muscle volume was maintained by increasing the limb and active muscle radius while decreasing the fibre length. The distance between the centre of the active muscle and the centre of the bone remained constant (30 mm, see Figure 3). The detection system remained halfway between the IZ and tendon region for all the simulations.

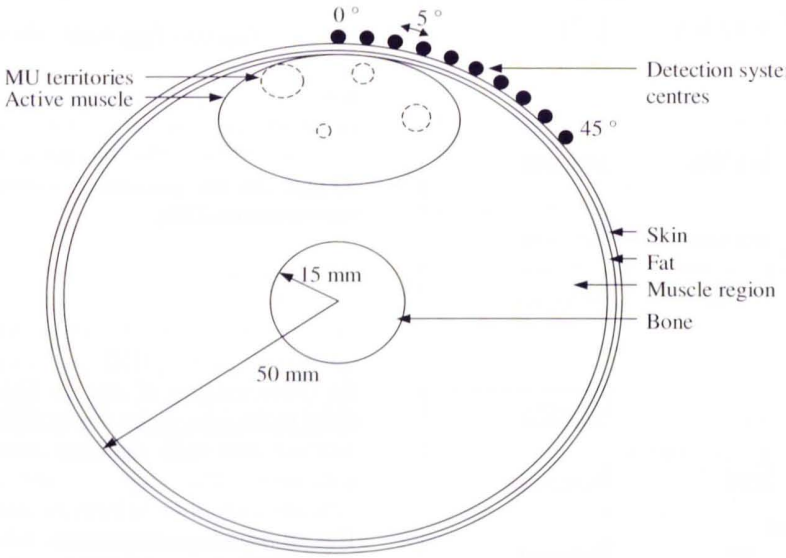

Figure 1: The model of the limb with different layers, the active muscle, the location and territory of the MUs. The location of the four detection system centres (see Figure 2) is also shown.

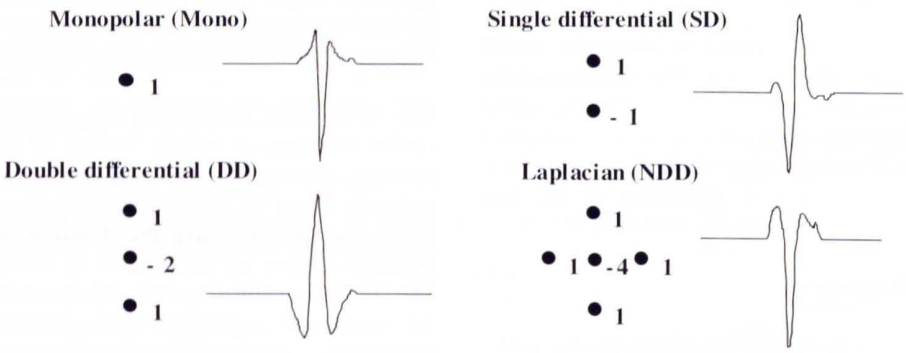

Figure 2: The spatial filters implemented in the simulation and an SFAP detected with each one.

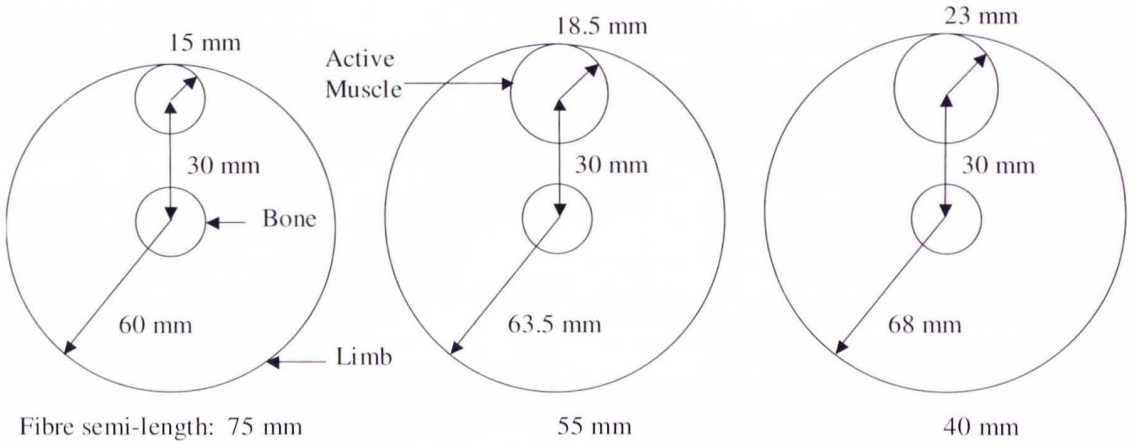

Figure 3: The muscle geometries used for incorporating muscle shortening. Increasing limb and muscle radius with decreasing muscle fibre length can be seen. The parameters describing the muscle geometry for library 1 (left), 2 (centre) and 3 (right) can be found in Table II.

Table II: Variable parameters used for simulating muscle shortening.

Library nr	Limb radius (mm)	Fibre semi-length (mm)	Muscle radius (A) (mm)	Width (w) (mm)	Radial distance between muscle fibre centres (mm)
1	60	75	15	83.29	0.29
2	63.5	55	18.5	49.58	0.31
3	68	40	23	30.99	0.34

The muscle shape was described by a Gaussian function (also called a bell-shaped curve), given in Equation 5:

$$r(z) = A \cdot \exp\left(\frac{-z^2}{2 \cdot w^2}\right) \tag{5}$$

where A defines the maximum radius of the active muscle, z is the longitudinal distance along the axis of the muscle and w defines the contraction width. The higher the value of w, the more contracted a muscle is. The relation between muscle volume and muscle shape is:

$$V = \int_{-d}^{d} \pi \cdot (r(z))^2 .dz \tag{6}$$

with d the muscle fibre semi-length. A muscle volume of 83.2 cm³ and maximum fibre semi-length of 75 mm was obtained from [20] and used for library 1 (the relaxed muscle). A fully contracted biceps brachii muscle can reduce its length to ½ of that in the relaxed state [20]. Library 3's fibre semi-length was thus selected as 40 mm, with library 2 given a value in-between the other two, see Table II.

The limb radius was obtained by adding all the radii of the components (bone, 30 mm spacing and active muscle). A numerical process was implemented to obtain the best values of muscle radius (A) and contraction width (w) to ensure a constant muscle volume. The complete process is described in [24]. The values obtained can be found in Table II. The fibre density decreases, because the number of fibres in the active muscle stays constant as the area increases. This is displayed by the increased radial distance between the fibre centres with increasing contraction force. CV distribution was Gaussian with mean 4 m/s and standard deviation 0.3 m/s [24].

2.7 Simulation of increased muscle force

Change in contraction force was modelled as a change in the number of recruited MUs, their discharge rate and CV. The active muscle is approximated by an ellipse with semi-axis lengths of a = 15 mm and b = 12.7 mm. These values were chosen to obtain the desired physiological cross-sectional area of 600 mm² for the biceps brachii as given by [20]. The limb radius used was 50 mm and the radial distance between muscle fibre centres 0.22 mm. The fibre semi-length was set to 60 mm.

Six simulations were performed in which the contraction force was increased from 10 to 100 % MVC. The force at which the entire MU pool was recruited was 85% MVC in all cases. For forces higher than 85% MVC, the increase in force is obtained by an increase in discharge rate only.

Table III: Variable parameters for simulating increasing contraction force.

Contraction force (% MVC)	Recruited Mus	Max discharge rate (pps)	Mean CV (m/s)	CV Std dev (m/s)
10	103	10.86	3.77	0.18
30	153	17.22	3.88	0.22
50	176	23.59	3.93	0.25
70	191	29.95	3.97	0.27
90	200	35	4	0.3
100	200	35	4	0.3

Since the smallest MU is recruited first, and CV is assigned increasing with MU size, the large MUs with high values of CV are not recruited at low values of contraction force. The result is a decrease in the mean CV with decreasing contraction force. This has been observed by several authors [26 - 28]. Table III shows the parameter values that were used in the simulations.

The discharge rate of each MU was computed from Equations 1 to 4. MUs with negative *RTE_time* values are not yet recruited at the time that the desired contraction strength is reached. Their discharge rate is thus set equal to zero.

The mean and standard deviation of CV is computed from a summation of the CV values assigned to the recruited MUs. From Table III the increase in CV with contraction force ranging from 10 to 50 % MVC is more significant than when the force increases above 50% MVC. This agrees with experimentally determined values of CV increase with contraction force [29].

When comparing the variables used for a 90 and 100 % MVC in Table III, the two simulations seem identical. The average discharge rate of the MUs will, however, be lower for a 90% contraction than for one of 100% MVC. The number of MUs discharging at the maximum rate of 35 pps will thus be lower for 90 % MVC than for 100% MVC.

3. RESULTS

All the graphs in this section are shown in normalised units (NU). Unless otherwise stated, they are normalised with respect to the value obtained at 0 °.

3.1 Effect of muscle shortening on crosstalk

Figure 4 shows the results obtained from the simulation of the three libraries. Library 1 (relaxed muscle) results in the most selective measurements, followed by library 2 and then 3. The only exception is NDD, where library 2 is more selective than library 1 at large distance.

NDD is the most selective filter at first for all three libraries, but right at the end DD increases beyond NDD in all the investigated cases.

Library 1 (relaxed muscle) results in the lowest values of MNF, followed by library 2 and then 3. At large distances library 3 has a lower MNF than library 2 for the DD and NDD detection systems.

The SD system always has the lowest MNF value. For libraries 1 and 2 NDD has the second lowest MNF values, but its values are then exceeded by those of DD. In the end the MNF of NDD is again lower than that of DD. For library 3, DD has a lower MNF than NDD right from the start, but NDD increases beyond DD's values at large distances.

NDD thus has the lowest MNF values for all three libraries at large distances. The last time its values exceed those of DD occurs at the same distance for all three libraries.

3.2 Effect of increased contraction force on crosstalk

Figure 5 shows the initial value of ARV and MNF as obtained with the different detection systems for different values of contraction force. ARV is strongly dependent on contraction force, while MNF varies only slightly when the contraction force increases. Both graphs are normalised with respect to the values obtained at 10 % MVC.

ARV increases with increasing contraction force. The increase can be explained by the fact that more MUs are recruited as the contraction force increases. Since an EMG signal is the summation of the contributions of all the active MUs, it should increase in amplitude as more MUs become active. The values measured at 25° (open markers) show a slightly larger increase than those measured at 0° (filled markers).

The MNF does not vary significantly with increasing contraction force. The variations do, however, appear to be very random in nature. This observation is independent of the circumferential position of the detection system. The same is thus seen at 0° and 25°.

Figure 6 shows the ARV and MNF values obtained from 10% and 100% MVC. The values for ARV and MNF obtained for the other contraction force strengths lay in-between the 10 and 100 % MVC results. The first observation is that neither the amplitude nor the frequency components of the various detection systems is largely affected by the difference in contraction force strength.

When comparing the ARV values, Mono, SD and DD show a very slight increase in selectivity with decreasing contraction force, while that of NDD remains constant.

The MNF values of Mono, SD and DD remain mostly unchanged for a 100% or 10% contraction. The decrease of NDD, DD and SD MNF with distance asymptotes at 30° for both values of contraction force, after which that of DD increases slightly. DD and NDD have slightly lower frequency components for 10% MVC as compared to 100% MVC.

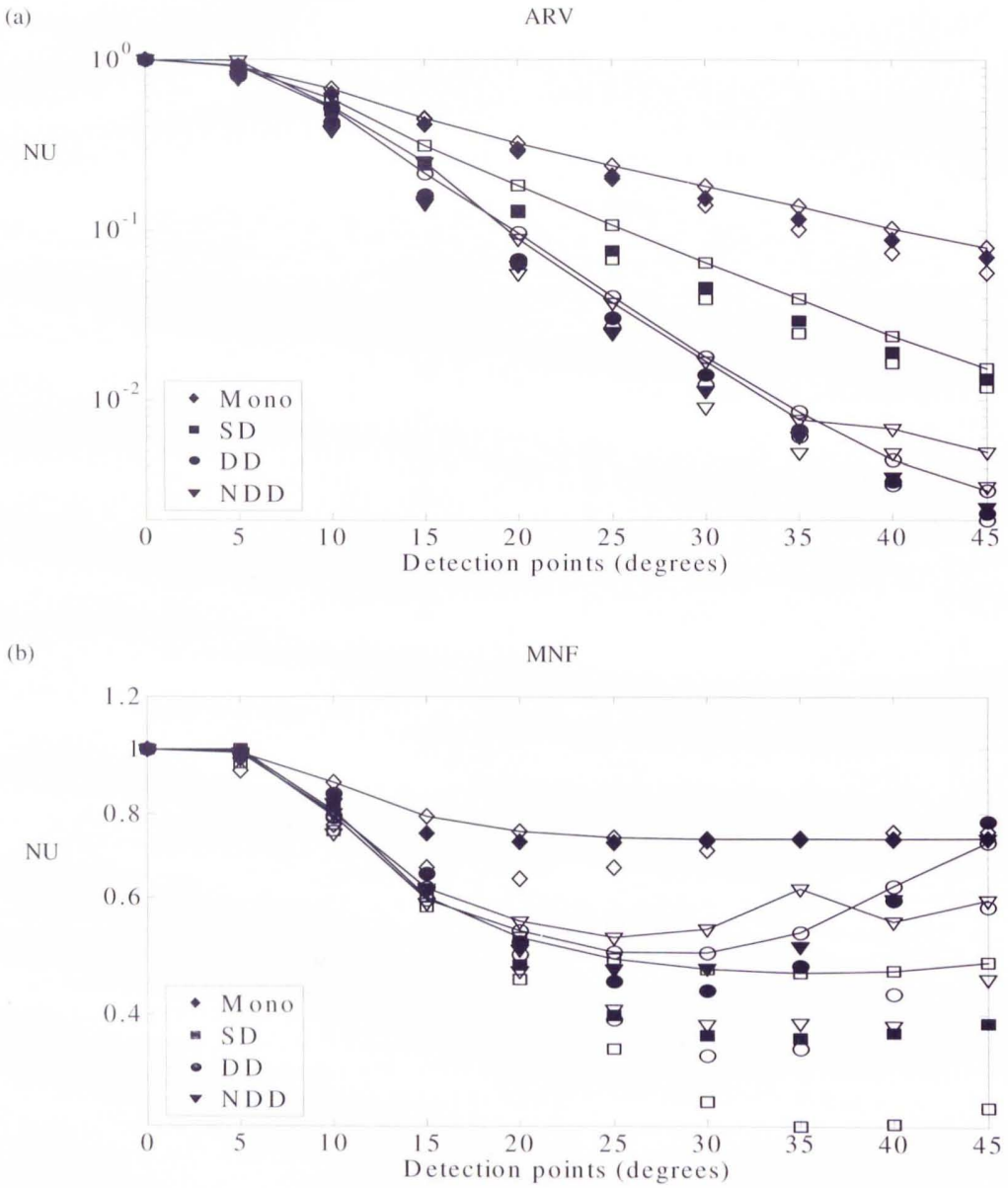

Figure 4: The ARV (a) and MNF (b) of libraries 1 (open markers, relaxed muscle), 2 (filled markers) and 3 (open markers with line, contracted muscle) with an IED of 5 mm, fat layer = 1 mm, skin conductivity = 1 S/m.

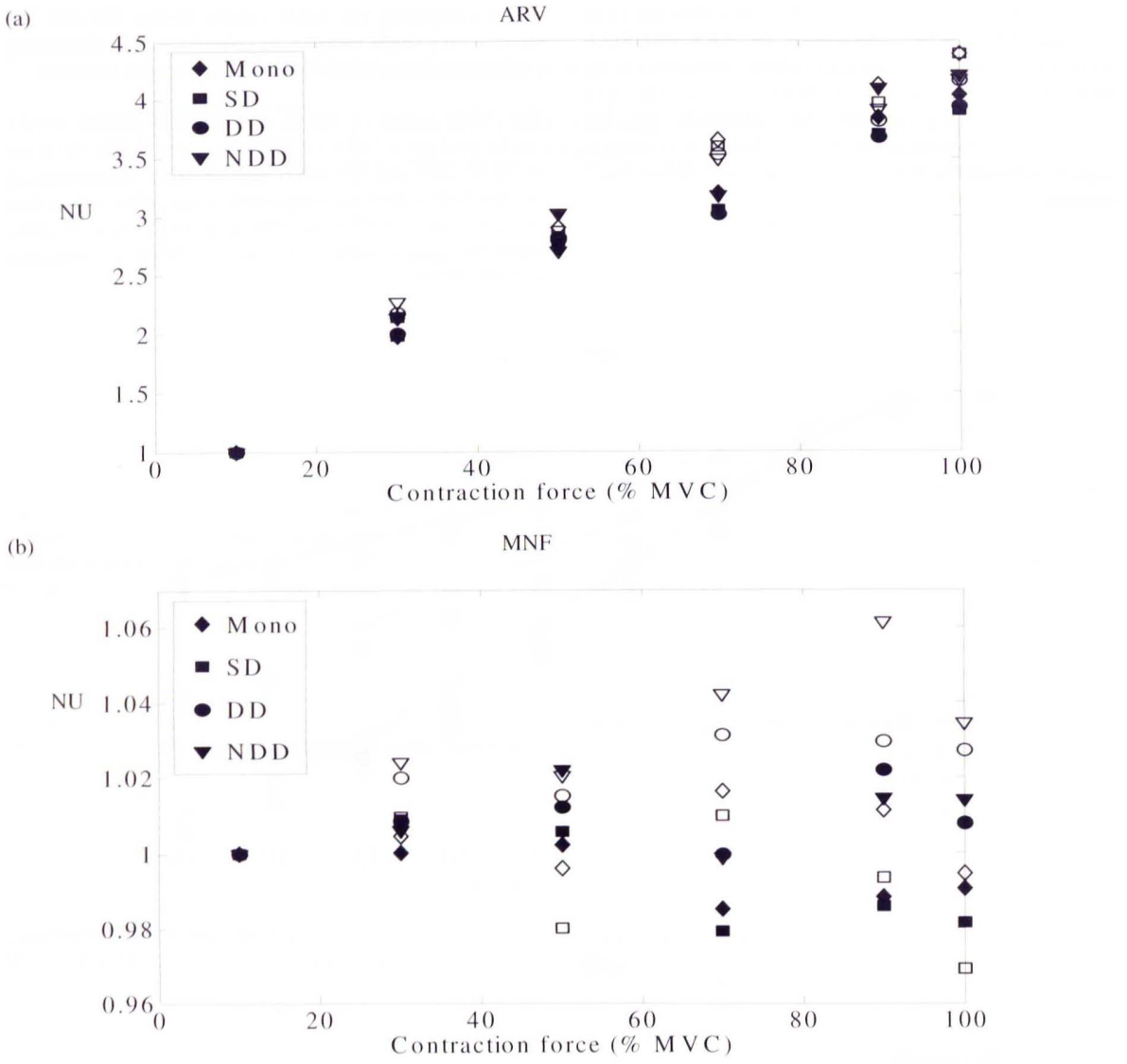

Figure 5: The initial values of ARV (a) and MNF (b) as detected at different contraction force levels at 0° (filled markers) and 25° (unfilled markers), fibre semi-length = 60 mm, fat layer = 1 mm, skin conductivity = 1 S/m, IED = 5 mm.

4. DISCUSSION

4.1 Effect of muscle shortening on crosstalk

The first objective of the simulation was to establish the relationship between limb geometry and amount of crosstalk. When a dynamic contraction is elicited, the muscle geometry changes along with other muscular properties (including CV, discharge rate and location of the IZ). Since these changes all occur simultaneously, it is very difficult to ascribe a change in the measured sEMG signal to a change in a single muscular property. By changing only the geometrical properties, the influence this has on crosstalk can be investigated directly.

When a muscle contracts the location of the IZ and tendon area can slide with respect to the skin and detection electrodes. It was shown by [29] that this sliding effect could result in EMG amplitude changes in excess of 200%. This may falsely be interpreted as an increase in muscle activity. A shift in biceps brachii IZ position of between 1 and 4 cm with changes in elbow angle was observed by [30], while [31] confirmed the fluctuations in EMG amplitude with changing knee angles. When an increase in amplitude is observed along with muscle shortening, it is thus not clear which part of the amplitude change is due to shifting of the IZ underneath the detection electrodes and which part (if

any) is due to the muscle shortening. A simulation enables one to change selected variables and keep the rest constant, investigating the individual effect of each variable on the output.

When shortening of the muscle fibre occurs, the IZ and tendon area move closer to the centre of the muscle. This means that the non-propagating components originate closer to the detection electrodes. The crosstalk can thus be expected to increase as the muscle fibres decrease in length. This is evident from Figure 4 where crosstalk is increased with decreased muscle length. However, the changes are relatively small, especially keeping in mind that the fibre length for the contracted muscle is reduced by almost half relative to that of the relaxed muscle. This could imply that the propagating wave components contribute significantly to the detected crosstalk.

Library 1 simulates a relaxed muscle, with the tendon area the furthest away from the detection electrodes. From Figure 4 it is clear that library 1 always results in the best crosstalk suppression, as expected. Furthermore

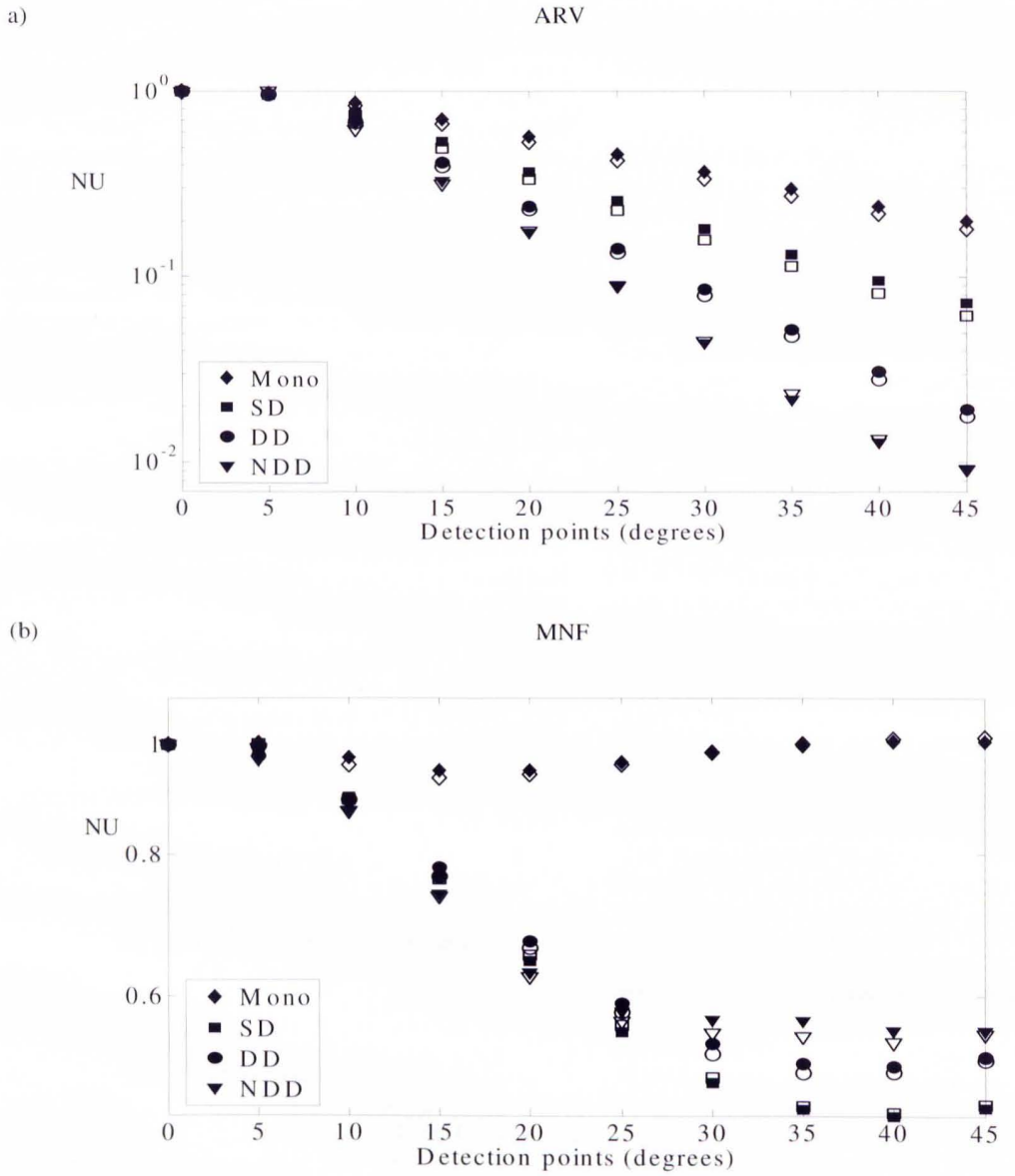

Figure 6: The ARV (a) and MNF (b) with a contraction force of 100 % (filled markers) and 10 % (open markers), fibre semi-length = 60 mm, fat layer = 1 mm, skin conductivity = 1 S/m, IED = 5 mm.

one would expect to see more crosstalk in library 2 and the most in library 3 (increasing crosstalk as the tendon area moves closer to the detection areas). This can be seen for the Mono, SD and DD systems, and also for most of NDD. At some stage, however, library 2 results in a more selective amplitude response than library 1 (NDD detected). This might be due to the decreasing fibre density with decreasing muscle length.

Increasing muscle length was linked to a decrease in spectral frequencies by [32] and [33], while [34] confirm that the non-propagating components will have a smaller influence with increasing muscle length because of the increased distance between the source and detection electrodes. As stated by [35], MNF estimates are greatly influenced by muscle fibre shortening and are also dependent on the detection system being used. This is clear from the variability of the MNF estimates in Figure 4 (b), especially for NDD.

4.3 Effect of increased contraction force on crosstalk

A similar study in which the contraction force was increased with the same steps as in the current study, and the ARV and MNF were experimentally determined was performed by [29]. The author reported that the influence of contraction force on the initial value of the MNF in the biceps brachii is small, and possibly masked by other factors. When comparing the results obtained by other authors on MNF and contraction force, it is difficult to draw any conclusion as the results vary quite a lot from one simulation to the next. MNF variation with contraction force increase depends on the muscle being studied, the IED and the transfer function of the underlying tissue layers [26]. A simulation study was done by [23] in which they found that MNF mostly increased and then remained constant with increasing contraction force. There were, however, exceptions. They conclude that a general relationship between spectral variables and MU recruitment cannot be defined.

For the current simulation (biceps brachii muscle, IED = 5 mm, skin layer = 1 mm and fat layer = 5 mm) the MNF does not vary significantly with increasing contraction force (see Figure 6 (b)). NDD is the most selective filter for crosstalk rejection for all of the contraction force strengths studied (Figure 6 (a)). It is clear that a change in the contraction force strength did not have a significant influence on either the amplitude or frequency components of the resulting EMG signals. This could also be as a result of the purely resistive nature of the model. According to Lowery et al. [36] the components in the model which could produce significant capacitive effects are the muscle tissue, fat layer and skin. Inclusion of capacitive effects in their model resulted in a phase shift of the detected action potentials with respect to the purely resistive model and a reduction in the amplitude of the non-propagating components. The thickness of the fat layer and skin are kept constant throughout the simulations and should thus have a relatively constant effect. However, the capacitive effects of the muscle tissue could influence the results since the thickness of the muscle tissue layer in the model changes. Limb geometry (i.e. realistic vs. cylindrical) is not expected to influence the results significantly since Lowery et al. [36] concluded that an idealized cylindrical limb model is adequate if the main parameters of interest are more qualitative features of the EMG signal, such as the approximate rate of decay of the EMG amplitude. Future research could thus focus on the inclusion of capacitive effects in the tissues.

5. CONCLUSIONS

The effects of two dynamic contraction parameters on crosstalk rejection were evaluated separately. A simulation model was used to investigate the effect of muscle shortening, and the effect of increased contraction force on crosstalk selectivity for four spatial filters. NDD resulted in marginally better crosstalk rejection in the increasing contraction force simulations. When muscle shortening was simulated, DD was the most selective for all the investigated situations, followed closely by NDD.

The MNF estimates of the EMG signal was clearly affected by muscle shortening and the accompanying geometrical changes, while increasing the contraction force did not cause a significant change in MNF. Generally, the ARV increased with muscle shortening as well as increasing muscle contraction force.

The selectivity of the detection systems was not significantly influenced by the variation in contraction force. This could be as a result of the purely resistive nature of the model. Assessment of crosstalk selectivity in dynamic contractions should thus, in future, include capacitive effects of the tissues.

ACKNOWLEDGEMENTS

This research has been supported by the National Research Foundation (South Africa) and the Italian Government under the Bilateral Research Agreement between South Africa and Italy.

6. REFERENCES

[1] C.J. De Luca and R. Merletti: "Surface myoelectric signal cross-talk among muscles of the leg", *Electroencephalography and clinical Neurophysiology* vol. 69, pp. 568-575, 1988.

[2] R. Merletti and P. Parker: "Electromyography", *Wiley Encyclopedia of Electrical and Electronics Engineering* vol. 6, pp. 524-540.

[3] D. Farina, R. Merletti, T. Indino and T. Graven-Nielsen: "Surface EMG crosstalk evaluated from experimental recordings and simulated signals. Reflections on crosstalk interpretation, quantification and reduction", *Methods of Information in Medicine* vol. 43, pp. 30-35, 2004.

[4] D. Farina, C. Cescon and R. Merletti: "Influence of anatomical, physical and detection-system parameters on surface EMG", *Biological Cybernetics* vol. 86, pp. 445-456, 2002.

[5] J.P.P. Van Vlugt and J.G. Van Dijk: "A convenient method to reduce crosstalk in surface EMG", *Clinical Neurophysiology* vol. 112, pp. 583-592, 2000.

[6] N.A. Dimitrova, G.V. Dimitrov and O.A. Nikitin: "Neither high-pass filtering nor mathematical differentiation of the EMG signals can considerably reduce cross-talk", *Journal of Electromyography and Kinesiology* vol. 12, pp. 235-246, 2002.

[7] D. Farina and A. Rainoldi: "Compensation of the effect of sub-cutaneous tissue layers on surface EMG: a simulation study", *Medical Engineering and Physics* vol. 21, pp. 487-496, 1999.

[8] M.M. Lowery, N.S. Stoykov and T.A. Kuiken: "A simulation study to examine the use of cross-correlation as an estimate of surface EMG cross talk", *Journal of Applied Physiology* vol. 94, pp. 1324-1334, 2003.

[9] D. Farina, R. Merletti, B. Indino, et al: "Surface EMG crosstalk between knee extensor muscles: experimental and model results", *Muscle & Nerve* vol. 26, pp. 681-695, 2002.

[10] T. Gootzen, D.F. Stegeman and A. Van Oosterom: "Finite limb dimensions and finite muscle length in a model for the generation of electromyographic signals", *Electroencephalography and clinical Neurophysiology* vol. 81, pp. 152-162, 1991.

[11] D.F. Stegeman, D. Dumitru, J.C. King, et al: "Near- and Far-Fields: Source Characteristics and the Conducting Medium in Neurophysiology", *American Clinical Neurophysiology Society* vol. 14, no. 5, pp. 429-442, 1997.

[12] D. Farina, L. Mesin, S. Martina, et al: "Comparison of spatial filter selectivity in surface myoelectric signal detection: influence of the volume conductor model", *Medical & Biological Engineering and Computing* vol. 42, pp. 114-120, 2004.

[13] D. Farina, L. Mesin, S. Marina and R. Merletti: "A surface EMG generation model with multilayer cylindrical description of the volume conductor", *IEEE Tansactions on Biomedical Engineering* vol. 51, no. 3, pp. 415-426, 2004.

[14] J.L. Orcholl, M. Scholar and J. Hudson: *Diagnostic criteria for the comparison of human and American black bear skeletal elements*, Available from: http://www.uwm.edu/Dept/Grad_Sch/McNair/Summer01/jackieorcholl.htm [Accessed 2004, March 29].

[15] X. Zhao, Y. Kinouchi, E. Yasuno, et al: "A new method for noninvasive measurement of multilayer tissue conductivity and structure using divided electrodes", *IEEE Transactions on Biomedical Engineering*, vol. 51, no. 2, pp. 362-370, 2004.

[16] D.G. Sale: *Strength training: Neural adaptation*, Department of Kinesiology, McMaster University, Hamilton, Canada, Available from: http://www.sportsci.org/encyc/drafts/Strength_neural_mech.doc, 2002 [Accessed: 2004, March, 29].

[17] C. Gabriel, S. Gabriel and E. Corthout: "The dielectric properties of biological tissues: I. Literature", *Physics in Medicine and Biology*, vol. 41, pp. 2231-2249, 1996.

[18] K.R. Foster and H.P. Swan: "Dielectrical properties of tissues", in *CRC Handbook of Biological Effects of Electromagnetic Field*, ed. C. P. Eds, CRC Press, pp. 26-95, 1986.

[19] L.A. Geddes and L.E. Baker: "The specific resistance of biological material - a compendium of data for the biomedical engineer and physiologist", *Medical & Biological Engineering and Computing*, vol. 5, pp. 271-293, 1967.

[20] B.A. Garner and M.G. Pandy: "Estimation of musculotendon properties in the human upper limb", *Annals of Biomedical Engineering*, vol. 31, pp. 207-220, 2003.

[21] S. Andreassen and L. Arendt-Nielsen: "Muscle fiber conduction velocity in motor units of the human anterior tibial muscle: a new size principle parameter", *Journal of physiology* vol. 391, pp. 561-571, 1987.

[22] A.J. Fuglevand, D.A. Winter and A.E. Patla: "Models of recruitment and rate coding organization in motor-unit pools", *Journal of Neurophysiology*, vol. 70 no.6, Dec, 1993.

[23] D. Farina, M. Fosci and R. Merletti: "Motor unit recruitment strategies investigated by surface EMG variables", *Journal of Applied Physiology* vol. 92, pp. 235-247, January, 2002.

[24] L. Mesin, M. Joubert, T. Hanekom, et al: "a Finite element model for describing the effect of muscle shortening on surface EMG", *accepted for publication: IEEE transactions on Biomedical Engineering*, Aug, 2005.

[25] W. Troni, R. Cantello and I. Tainero: "Conduction velocity along human muscle fibers in situ", *Neurology* vol. 33, pp. 1453-1459, 1983.

[26] J.Y. Hogrel, J. Duchene and J.F. Marini: "Variability of some sEMG parameter estimates with electrode location", *Journal of Electromyography and Kinesiology* vol. 8, pp. 305-315, 1998.

[27] T. Masuda and C.J. De Luca: "Recruitment threshold and muscle fiber conduction velocity of single motor units", *Journal of Electromyography and Kinesiology* vol. 1, no. 2, pp. 116-123, 1991.

[28] R. Merletti, A. Rainoldi and D. Farina: "Surface electromyography for noninvasive characterization of muscle", *Exercise and Sport Science Review* vol. 29, no. 1, pp. 20-25, 2001.

[29] A. Rainoldi, G. Galardi, L. Maderna, et al: "Repeatability of surface EMG variables during voluntary isometric contractions of the biceps brachii muscle", *Journal of Electromyography and Kinesiology* vol. 9, pp. 105-119, 1999.

[30] K. Saitou, M. Okada and T. Sadoyama: "Effect on surface EMG waveforms of electrode location with respect to the neuromuscular junctions: its significance in EMG-muscle length relation", *Proceedings of the 8th Congress of ISEK* vol. Baltimore, pp. 27-30, 1990.

[31] G.M. Ghori, B. Donne and R.G. Luckwill: "Relationship between torque and EMG activity of a knee extensor muscle during isokinetic concentric and eccentric actions", *Journal of Electromyography and Kinesiology* vol. 5, no. 2, pp. 109-115, 1995.

[32] M. Okada: "Effect of muscle length on surface EMG wave forms in isometric contractions", *European journal of applied physiology and occupational physiology* vol. 56, no. 4, pp. 482-486, 1987.

[33] N.A. Dimitrova, G.V. Dimitrov and Z.C. Lateva: "Influence of the fiber length on the power spectra of single muscle fiber extracellular potentials", *Electromyography and clinical Neurophysiology* vol. 31, no. 7, pp. 387-398, 1991.

[34] G. Kamen and G.E. Caldwell: "Influences of muscle length on the EMG signals", *Physiology and Interpretation of the Electromyogram* vol. 13, no. 5, pp. 366-384, 1996.

[35] E. Schulte, D. Farina, R. Merletti, et al: "Influence of muscle fibre shortening on estimates of conduction velocity and spectral frequencies from surface electromyographic signals", *Medical & Biological Engineering and Computing* vol. 42, pp. 477-486, 2004.

[36] M.M. Lowery, N.S. Stoykov, J.P.A. Dewald, et al: "Volume conduction in an anatomically based surface EMG model", *IEEE Transactions on Biomedical Engineering*, vol. 51, no. 12, Dec, 2004.

VOL 98 No 2
June 2007

SAIEE Africa Research Journal